Turk J Elec Engin, VOL.16, NO.3 2008, © TÜBİTAK

Distance Relaying Algorithm for Double-Circuit Transmission Line with Compensation for Reactance Effect under Standard Availability of Measurements

Jan IZYKOWSKI, Marcin BOZEK
Wroclaw University of Technology Institute of Electrical Power Engineering
Wybrzeze Wyspianskiego 27 50-370 Wroclaw-POLAND
e-mail: jan.izykowski@pwr.wroc.pl • marcin.bozek@pwr.wroc.pl

Abstract

This paper deals with non-pilot distance protection of a double-circuit transmission line. Negative impact of the reactance effect, appearing in measuring a fault loop impedance, on operation of the relay is discussed. An adaptive algorithm allowing one to prevent the relay from mis- or mal-operation caused by the reactance effect is introduced. The algorithm is designed for a standard availability of measurements from one end of the double-circuit line, i.e. when three-phase voltage and current from the faulted line circuit, and additionally zero-sequence current from the healthy line circuit, are provided as the relay input signals. The algorithm is based on changing the position of the distance relay characteristic in such a way that the reactance effect is effectively compensated for. For this purpose the shift vector is determined in on-line relatively simple calculations. The delivered adaptive algorithm has been tested using current and voltage signals obtained from simulation of varies faults using the ATP-EMTP software program. Selected results of the evaluation are presented.

Key Words: *Double-circuit transmission line, distance protection, fault, fault loop impedance measurement, reactance effect, adaptive characteristic.*

1. Introduction

The principle of distance relaying is well known and is based on comparing the measured fault loop impedance with a characteristic adequately shaped on the impedance plane. This rule could fail in case of presence of high fault resistance at the fault [1–6]. A combined effect of fault resistance and pre-fault power flow may cause the relay not to trip for faults within the protective zone, or may lead to inadvertent operation for faults outside the zone [4–6]. This is so since fault resistance is seen from the relay location as certain apparent impedance, thus with the contents of the reactance. This effect, called as the reactance effect, influences the fault loop impedance measurement of the distance relay and thus its performance.

To compensate for the negative impact of the reactance effect, adaptive algorithms may be used in a decision unit of the distance relay. This paper introduces such adaptive algorithm. It is based on on-line calculating components of the shift vector $\Delta \underline{Z}$, according to measured voltage and current. The relay characteristic position on $R - X$ plane is not constant, but is shifted according to the shift vector $\Delta \underline{Z}$

value. Since tripping time is essential in the first protective zone, calculations are relatively simple, thus not requiring time-consuming operations.

Figure 1 presents a schematic diagram of the analysed transmission network with the double-circuit transmission line. The faulted line is connected between buses AA, BA, while the healthy line lies between buses AB, BB. At both line ends there are the equivalent systems represented, with electromotive forces and internal source impedances. The delivered adaptive algorithm utilizes the standard availability of the measured signals as depicted in Figure 1. In this case the distance relay is supplied with three-phase current $\underline{I}_A$ and voltage $\underline{V}_A$ from the faulted line and zero-sequence current from the healthy line $\underline{I}_{AB0}$.

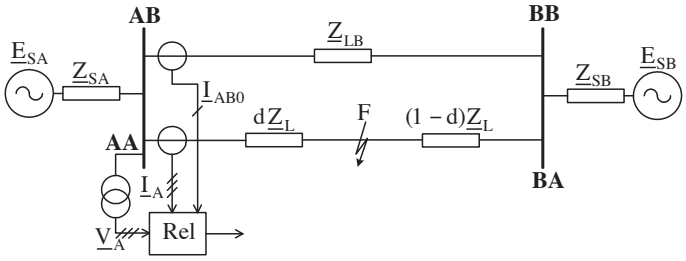

Figure 1. Schematic diagram of analysed transmission network.

2. Basics of the Adaptive Algorithm

One of the main features of digital distance relays in present use is the ease with which one can apply various decision algorithms. Therefore, it is possible to implement adaptive procedures to standard decision algorithms to make the relay more attuned to system fault conditions.

The adaptive algorithm introduced in this paper is based on the generalized fault loop model [5], which is stated as

$$\underline{V}_{Ap} - d\underline{Z}_{1L}\underline{I}_{Ap} - R_F\underline{I}_F = 0 \tag{1}$$

where

$$\underline{V}_{Ap} = \underline{a}_1\underline{V}_{A1} + \underline{a}_2\underline{V}_{A2} + \underline{a}_0\underline{V}_{A0}$$

is the fault loop voltage;

$$\underline{I}_{Ap} = \underline{a}_1\underline{I}_{AA1} + \underline{a}_2\underline{I}_{AA2} + \underline{a}_0\frac{\underline{Z}_{0L}}{\underline{Z}_{1L}}\underline{I}_{AA0} + \underline{a}_0\frac{\underline{Z}_{0m}}{\underline{Z}_{1L}}\underline{I}_{AB0}$$

is the fault loop current; d is distance to fault [p.u.]; R_F is fault path resistance; $\underline{I}_F = \underline{a}_{F1}\underline{I}_{F1} + \underline{a}_{F2}\underline{I}_{F2} + \underline{a}_{F0}\underline{I}_{F0}$ is total fault current; $\underline{Z}_{1L}$, $\underline{Z}_{0L}$ are positive- and zero-sequence line impedances, respectively; and $\underline{Z}_{0m}$ is the mutual coupling zero-sequence line impedance.

The fault loop voltage and current involved in (1) are expressed in terms of the symmetrical components of the measured signals. The subscript i denotes the sequence component type: $i = 1$ is for positive-sequences, $i = 2$ is for negative-sequences, and $i = 0$ is for zero-sequences. The coefficients $\underline{a}_i$ determine fault loop signals adequately to the fault type as shown in Table 1. Fault types are denoted with names of faulted phases (a, b, c), and additionally for faults involving ground the letter 'g' is included.

Table 1. Coefficients $\underline{a}_i$ for determining fault loop signals from (1).

Fault type	$\underline{a}_1$	$\underline{a}_2$	$\underline{a}_0$
a–g	1	1	1
b–g	$\underline{a}^2$	$\underline{a}$	1
c–g	$\underline{a}$	$\underline{a}^2$	1
a–b, a–b–g, a–b–c, a–b–c–g	$1-\underline{a}^2$	$1-\underline{a}$	0
b–c, b–c–g	$\underline{a}^2-\underline{a}$	$\underline{a}-\underline{a}^2$	0
c–a, c–a–g	$\underline{a}-1$	$\underline{a}^2-1$	0
$\underline{a} = \exp(\mathrm{j}2\pi/3)$			

To determine the voltage drop across the fault path resistance, one needs to establish weighting coefficients $\underline{a}_{Fi}$. These coefficients can be derived by considering the boundary conditions for a particular fault type. There is a certain freedom for that and one can derive alternative sets of the coefficients. The values of the weight coefficients used further are gathered in Table 2. It is distinctive that, for the zero-sequence, we have $\underline{a}_{F0} = 0$, which is advantageous since use of the zero-sequence line impedance, considered as an unreliable parameter, is avoided in the calculations.

Table 2. Alternative sets of weighting coefficients $\underline{a}_{Fi}$ with $\underline{a}_{F0}=0$.

Fault type	Set I		Set II		Set III	
	$\underline{a}_{F1}$	$\underline{a}_{F2}$	$\underline{a}_{F1}$	$\underline{a}_{F2}$	$\underline{a}_{F1}$	$\underline{a}_{F2}$
a-g	0	3	3	0	1.5	1.5
b-g	0	$3\underline{a}$	$3\underline{a}^2$	0	$1.5\ \underline{a}^2$	$1.5\ \underline{a}$
c-g	0	$3\underline{a}^2$	$3\underline{a}$	0	$1.5\ \underline{a}$	$1.5\ \underline{a}^2$
a-b	0	$1-\underline{a}$	$1-\underline{a}^2$	0	$\frac{1-\underline{a}^2}{2}$	$\frac{1-\underline{a}}{2}$
b-c	0	$\underline{a}-\underline{a}^2$	$\underline{a}^2-\underline{a}$	0	$\frac{\underline{a}^2-\underline{a}}{2}$	$\frac{\underline{a}-\underline{a}^2}{2}$
c-a	0	$\underline{a}^2-1$	$\underline{a}-1$	0	$\frac{\underline{a}-1}{2}$	$\frac{\underline{a}^2-1}{2}$
a-b-g	$1-\underline{a}^2$	$1-\underline{a}$	$1-\underline{a}^2$	$1-\underline{a}$	$1-\underline{a}^2$	$1-\underline{a}$
b-c-g	$\underline{a}^2-\underline{a}$	$\underline{a}-\underline{a}^2$	$\underline{a}^2-\underline{a}$	$\underline{a}-\underline{a}^2$	$\underline{a}^2-\underline{a}$	$\underline{a}-\underline{a}^2$
c-a-g	$\underline{a}-1$	$\underline{a}^2-1$	$\underline{a}-1$	$\underline{a}^2-1$	$\underline{a}-1$	$\underline{a}^2-1$
a-b-c, a-b-c-g	$1-\underline{a}^2$	0	$1-\underline{a}^2$	0	$1-\underline{a}^2$	0

The popular circle characteristic of MHO type (this name comes from writing OHM backward) is taken for further considerations; however the presented method can be applied to other characteristic shapes as well. The MHO characteristic with a boundary of the first zone set to 85% of the protected line length ($s = 0.85$ p.u.) is described by the inequality

$$\left(R_{AP} - 0.5sR_{1L}\right)^2 + \left(X_{Ap} - 0.5sX_{1L}\right)^2 \leq \left(0.5s\,|\underline{Z}_{1L}|\right)^2, \tag{2}$$

where R_{Ap} is the fault loop resistance measured by the relay, X_{Ap} is the fault loop reactance measured by the relay, R_{1L} is the positive sequence resistance of the whole protected line, X_{1L} is the positive sequence reactance of the whole protected line, and $\underline{Z}_{1L} = R_{1L}+\mathrm{j}X_{1L}$ is positive sequence impedance of the whole protected line.

The inequality (2) defines the interior part of the circle characteristic, for which the centre is located at the point $(0.5sR_{1L}, 0.5sX_{1L})$ and the radius is equal to: $0.5s|\underline{Z}_{1L}|$. This standard characteristic may be modified by introducing the components of the $\Delta\underline{Z}$ shift vector. As a result of introducing the shift vector,

one obtains the adaptive MHO characteristic as

$$(R_{Ap} - (0.5sR_{1L} + \Delta R))^2 + (X_{Ap} - (0.5sX_{1L} + \Delta X))^2 \leq (0.5s\,|\underline{Z}_{1L}|)^2\,, \tag{3}$$

where $\Delta R$and ΔX denote the resistive and reactive components of the shift vector of the relay characteristic. This allows for compensating for the reactance effect, which makes the relay invulnerable to presence of fault resistance. A way of calculating components of the shift vector of the relay characteristic is presented in section 3.

3. Determination of Shift Vector

Expressing the fault loop model (1) in terms of impedances, one obtains

$$\underline{Z}_{Ap} - d\underline{Z}_{1L} - R_F\frac{\underline{I}_F}{\underline{I}_{Ap}} = 0, \tag{4}$$

where

$$\underline{Z}_{Ap} = \frac{\underline{V}_{Ap}}{\underline{I}_{Ap}} = R_{Ap} + jX_{Ap}$$

is the fault loop impedance.

The third component on the left side of (1) presents the error in measured fault loop impedance. In order to consider the compensation for this error, equation (4) is rewritten in the form

$$\underline{Z}_{Ap} = d\underline{Z}_{1L} + \Delta\underline{Z}, \tag{5}$$

where $\Delta\underline{Z} = \Delta R + j\Delta X = R_F\left(\underline{I}_F/\underline{I}_{Ap}\right)$ is the error due to resistance of a fault path resistance.

According to (5), the fault loop impedance measured by a standard distance relay is a sum of the correct value $d\underline{Z}_{1L}$ and the error value $\Delta\underline{Z}$. In order to compensate for this error, the fault loop impedance measuring algorithm of the relay is considered as unchanged, i.e. as in the standard distance relay, however, the adaptation is introduced into the decision making algorithm of the relay. This is performed by shifting the position of the relay characteristic on the impedance plane by the shift vector: ΔR for the resistance and ΔX for the reactance. Determination of the required shifts follow.

Determination of the shift vector $\Delta\underline{Z}$ requires calculating the total fault current $\underline{I}_F$. For this purpose the weighting coefficients set with $\underline{a}_{F0} = 0$ (as in Table 2) is chosen and thus one gets

$$\underline{I}_F = \underline{a}_{F1}\underline{I}_{F1} + \underline{a}_{F2}\underline{I}_{F2}. \tag{6}$$

Unknown components of the total fault current $\underline{I}_{F1}$ and $\underline{I}_{F2}$ can be derived from the equivalent circuit diagrams for the positive- and negative-sequence [5]. The equations resulting from the equivalent circuit diagrams of the network shown in Figure 1 are

$$\underline{I}_{F1} = \frac{\Delta\underline{I}_{A1}}{\underline{k}_F} \tag{7}$$

$$\underline{I}_{F2} = \frac{\underline{I}_{A2}}{\underline{k}_F}, \tag{8}$$

where $\Delta \underline{I}_{A1}$ is the incremental positive-sequence current, $\underline{I}_{A2}$ is the negative-sequence current, $\underline{k}_F$ is the fault current distribution factor (identical for both sequences).

The fault current distribution factor depends on the line configuration and for the considered transmission network from Figure 1 takes the form

$$\underline{k}_F = \frac{\underline{K}_1 d + \underline{L}_1}{\underline{M}_1}, \tag{9}$$

where $\underline{K}_1 = -\underline{Z}_{1L}(\underline{Z}_{1SA} + \underline{Z}_{1SB} + \underline{Z}_{1LB})$, $\underline{L}_1 = \underline{Z}_{1L}(\underline{Z}_{1SA} + \underline{Z}_{1SB} + \underline{Z}_{1LB}) + \underline{Z}_{1LB}\underline{Z}_{1SB}$, and $\underline{M}_1 = \underline{Z}_{1L}\underline{Z}_{1LB} + (\underline{Z}_{1L} + \underline{Z}_{1LB})(\underline{Z}_{1SA} + \underline{Z}_{1SB})$.

In particular, the fault current distribution factor (9) is a function of the unknown distance to fault (d, [p.u.]) and the immeasurable (in case of one end measurements) value of the remote source impedance $\underline{Z}_{1SB}$. However, it will be further shown that it is not necessary to determine the value of $\underline{k}_F$.

Taking into account (6)–(8), the generalized fault loop model (1) takes the form

$$\underline{V}_{Ap} - d\underline{Z}_{1L}\underline{I}_{Ap} - R_F \frac{\underline{a}_{F1}\Delta \underline{I}_{A1} + \underline{a}_{F2}\underline{I}_{A2}}{\underline{k}_F} = 0. \tag{10}$$

In general, the fault current distribution factor $\underline{k}_F$ is a complex number and it may be presented as

$$\underline{k}_F = k_F e^{j\gamma} = k_F \left(\cos\gamma + j \sin\gamma\right), \tag{11}$$

where k_F is the magnitude and γ is the angle of the fault current distribution factor.

Substituting (11) into (10) and then dividing by the fault loop current $\underline{I}_{Ap}$ gives

$$\underline{Z}_{Ap} - d\underline{Z}_{1L} - \frac{R_F}{k_F}\underline{N}_{12} e^{-j\gamma} = 0 \tag{12}$$

where $\underline{N}_{12} = N_{12}^{real} + jN_{12}^{imag} = \frac{\underline{a}_{F1}\Delta \underline{I}_{A1} + \underline{a}_{F2}\underline{I}_{A2}}{\underline{I}_{Ap}}$ is the ratio of the total fault current (6) and the fault loop current defined in (1).

After resolving $\underline{N}_{12}$ into the real and imaginary parts, equation (12) takes the form

$$\underline{Z}_{Ap} - d\underline{Z}_{1L} - \frac{R_F}{k_F}\left(G_{12}^{real} + jG_{12}^{imag}\right) = 0, \tag{13}$$

where

$$G_{12}^{real} = N_{12}^{real}\cos\gamma + N_{12}^{imag}\sin\gamma$$
$$G_{12}^{imag} = N_{12}^{imag}\cos\gamma - N_{12}^{real}\sin\gamma.$$

Comparing equation (13) with equation (5) results in obtaining the ratio of the components of the shift vector:

$$\frac{\Delta R}{\Delta X} = \frac{G_{12}^{real}}{G_{12}^{imag}} = \frac{N_{12}^{real}\cos\gamma + N_{12}^{imag}\sin\gamma}{N_{12}^{imag}\cos\gamma - N_{12}^{real}\sin\gamma}. \tag{14}$$

It is justified to assume $\gamma = 0$, because in real transmission networks the angle of the fault current distribution factor is close to zero (Figure 2) and rarely exceeds 10^o [2]. As a result, a simplified form of equation (14) is obtained:

$$\frac{\Delta R}{\Delta X} = \frac{N_{12}^{real}}{N_{12}^{imag}}. \tag{15}$$

From equations (5) and (15) one may derive the components of the shift vector, which are

$$\Delta R = \frac{N_{12}^{real}\left(R_{Ap}X_{1L} - X_{Ap}R_{1L}\right)}{N_{12}^{real}X_{1L} - N_{12}^{imag}R_{1L}} \tag{16}$$

$$\Delta X = \frac{N_{12}^{imag}\left(R_{Ap}X_{1L} - X_{Ap}R_{1L}\right)}{N_{12}^{real}X_{1L} - N_{12}^{imag}R_{1L}}. \tag{17}$$

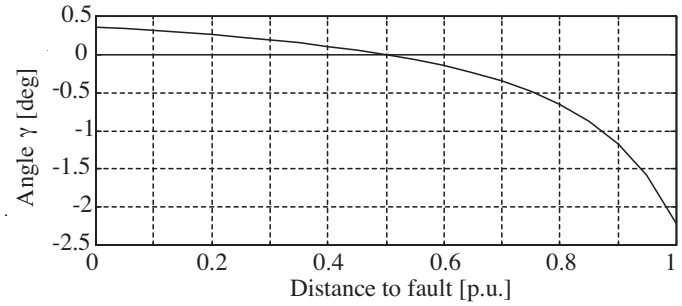

Figure 2. Plot of angle γ as function of distance to fault (determined for the transmission network defined in Table 3).

4. ATP-EMTP Evaluation

The derived adaptive algorithm has been thoroughly tested and evaluated using signals taken from ATP-EMTP [7] simulations. The modelled transmission network comprised of a 400 kV transmission line and two equivalent systems. Parameters of the network are gathered in Table 3.

The resultant data of the ATP-EMTP simulations (the pl4 files) was transferred into the Matlab program, where measurement and decision making algorithms of the standard, and the presented adaptive distance relays were programmed. The signals were sampled at 1000 Hz sampling frequency and standard full-cycle Fourier filtration was applied to determine the phasors of the processed signals. By having phasors for the three-phase voltages and currents, phasors for the symmetrical components were also determined. Utilising the determined phasors, the fault loop impedance measurement was performed, and also the required shift of the adaptive MHO characteristic was determined.

Presented evaluation results include line-to-earth faults, as these faults stand for approximately 70% of all faults in transmission and distribution lines. Various fault locations and fault resistances ranging from 0.1 Ω up to 20 Ω have been taken in modelling, in order to determine efficiency of the proposed algorithm.

Table 4 shows a comparison between the standard (the MHO characteristic has a fixed position) and the adaptive (the MHO characteristic undergoes shifting) distance relays. Tripping time, determined when for three consecutive samples there is encroachment of the MHO characteristic by the fault loop impedance trajectory, for both relays is presented. For example, in case of fault resistance: $R_F = 10\ \Omega$ the reach of the first zone of the standard relay is up to 0.60 p.u., while of the adaptive relay up to the set value equal to 0.85 p.u. Moreover, the tripping time of the adaptive relay is faster than for the standard relay.

Table 3. Parameters of modelled transmission network.

System element	Parameter	
Double-circuit line	Length, l	150 km
	$\underline{Z}'_{1L}$	(0.0276 + j0.315) Ω/km
	$\underline{Z}'_{0L}$	(0.275 + j1.0265) Ω/km
	$\underline{C}'_{1L}$	13 nF/km
	$\underline{C}'_{0L}$	8.5 nF/km
	$\underline{C}'_{0m}$	5.5 nF/km
	$\underline{Z}'_{0m}$	(0.20 + j0.628) Ω/km
Equivalent system A	$\underline{Z}_{1SA}$	(2.615+ j14.829) Ω
	$\underline{Z}_{0SA}$	(4.637 + j26.297) Ω
	Voltage phase	-30^o
Equivalent system B	$\underline{Z}_{1SB}$	$\underline{Z}_{1SB} = \underline{Z}_{1SA}$
	$\underline{Z}_{0SB}$	$\underline{Z}_{0SB} = \underline{Z}_{0SA}$
	Voltage phase	0^o

Table 4. Tripping signal and tripping time for various fault resistance values.

d [p.u.]	$R_F = 10\ \Omega$				$R_F = 20\ \Omega$			
	Standard relay		Adaptive relay		Standard relay		Adaptive relay	
	Trip. signal	Trip. time [ms]	Trip. signal	Trip. time [ms]	Trip. signal	Trip. time [ms]	Trip. signal	Trip. time [ms]
0.10	1	9	1	7	1	15	1	10
0.15	1	9	1	8	1	15	1	11
0.20	1	13	1	11	1	16	1	12
0.25	1	13	1	12	1	16	1	13
0.30	1	16	1	14	1	17	1	13
0.35	1	15	1	13	1	18	1	14
0.40	1	17	1	15	0	–	1	14
0.45	1	16	1	15	0	–	1	15
0.50	1	19	1	16	0	–	1	17
0.55	1	19	1	16	0	–	1	17
0.60	1	25	1	17	0	–	1	20
0.65	0	–	1	18	0	–	1	22
0.70	0	–	1	19	0	–	1	24
0.75	0	–	1	21	0	–	1	26
0.80	0	–	1	23	0	–	1	28
0.85	0	–	1	31	0	–	1	32
0.90	0	–	0	–	0	–	0	–

In figures 3–9 are investigation results, considering an a-g fault type at fault distance $d = 0.8$ p.u., with fault resistance R_F=10 Ω. The input signals of the relay are shown in Figures 3–5. Figure 6 presents tripping signal for the standard and adaptive relays. Note that there is no tripping for the standard relay, while the wanted tripping for the adaptive relay. Figure 7 shows the measured fault loop impedance $\underline{Z}_{Ap}$ trajectory, standard and adaptive (only for the post-fault steady state) distance relay MHO characteristics. In Figures 8–9 the calculated samples of the resistive ΔR and reactive ΔX shifts of the adaptive characteristic are shown.

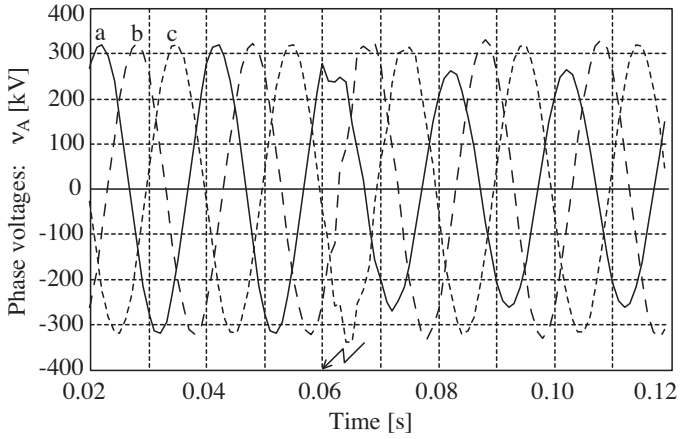

Figure 3. Example: phase voltages from faulted line at the relaying point.

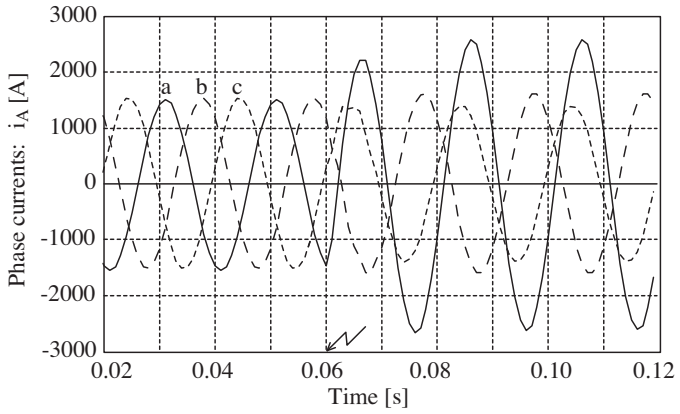

Figure 4. Example: phase currents from faulted line at the relaying point.

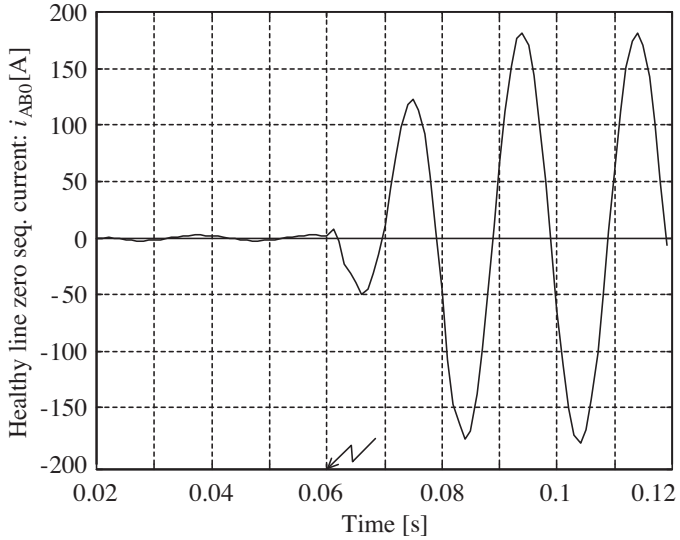

Figure 5. Zero sequence current from the healthy line at the relaying point.

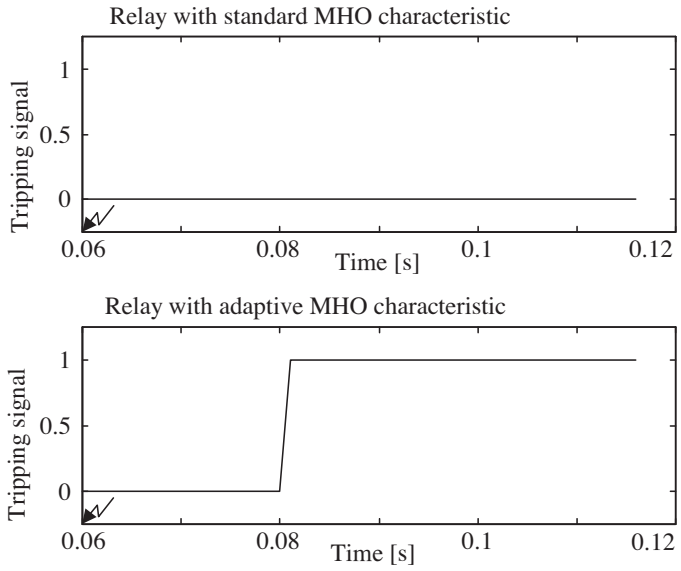

Figure 6. Example: tripping signal for standard and adaptive relay.

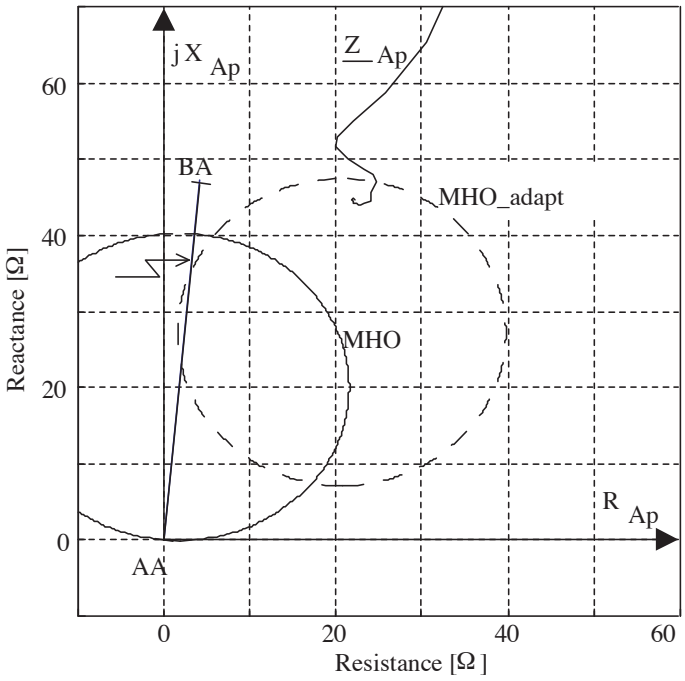

Figure 7. Example: fault loop impedance ($\underline{Z}_{Ap}$) trajectory, distance relay MHO characteristics: standard and adaptive (at the post-fault steady state).

5. Conclusion

This paper introduces an adaptive algorithm that allows shifting the relay impedance characteristic on $R-X$ plane, according to on-line calculated value of the shift vector. It allows one to compensate for the negative influence of the reactance effect in the fault loop measurement. Additionally, the algorithm speeds up taking a tripping decision.

The components of the shift vector are functions of locally measured quantities, line parameters and fault type. Thus, the equations determining these components are simple in form and do not require sophisticated calculations. This is important in that it is not necessary to provide data from the remote end of the protected line and the source impedances, which makes the algorithm easy to implement in a digital distance protective relay.

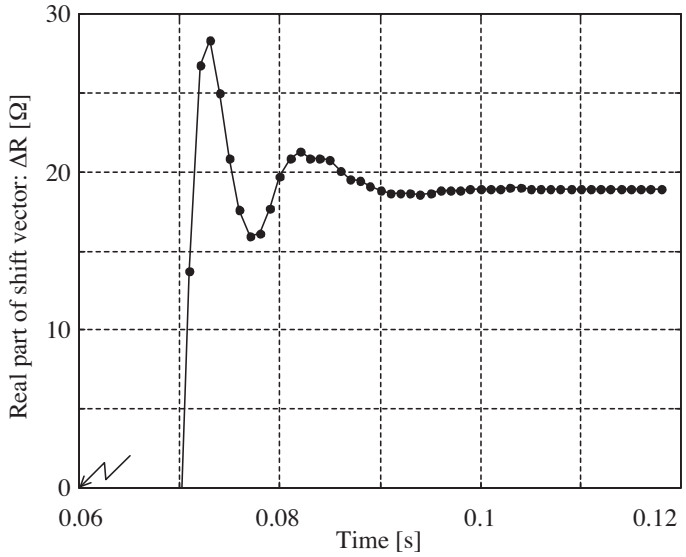

Figure 8. Example: calculated resistive shift ΔR of the adaptive characteristic.

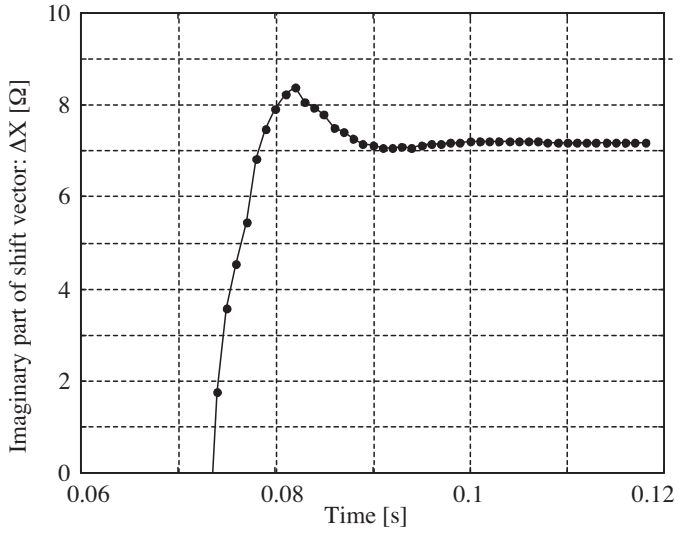

Figure 9. Example: calculated reactive shift ΔX of the adaptive characteristic.

Evaluation utilizing ATP–EMTP simulations proved that incorporating the presented adaptive algorithm enhances operation of the distance relay, making the relay practically invulnerable to reactance effect within wide range of fault specifications. It is also highly desirable for future investigations to apply the real system measurement data for testing the proposed adaptive algorithm.

Further study should take into account the case with no measurements from the healthy line circuit available for the distance relay input signals.

Acknowledgment

This work was supported in part by the Ministry of Science and Higher Education of Poland under Grant N511 008 32/1688.

References

[1] J. Izykowski, E. Rosolowski, M. M. Saha, "Postfault analysis of operation of distance protective relays of power transmission lines", IEEE Transactions on Power Delivery, Vol. 22, No. 1, pp. 74–81, 2007.

[2] A. Wiszniewski, "Accurate fault impedance locating algorithm", IEE Proceedings, Vol. 130, Pt. C, No. 6, pp. 311–315, 1983.

[3] L. Eriksson, M. M. Saha, G. D. Rockefeller, "An accurate fault locator with compensation for apparent reactance in the fault resistance resulting from remote-end infeed", IEEE Transactions on Power Apparatus and Systems, Vol. PAS–104, No.2, pp. 424–436, 1985.

[4] Y. Liao, S. Elangovan, "Digital distance relaying algorithm for first zone protection for parallel transmission lines", IEE Proceedings: Generation, Transmission and Distribution, Vol. 145, No. 5, pp. 531–536, 1998.

[5] J. Izykowski, E. Rosolowski, M. M. Saha, "Locating faults in parallel transmission lines under availability of complete measurements at one end", IEE Proceedings: Generation, Transmission and Distribution, Vol. 151, No. 2, pp. 268–273, 2004.

[6] Yi Hu, D. Novosel, M. M. Saha, V. Leitloff, "An adaptive scheme for parallel-line distance protection", IEEE Transactions on Power Delivery, Vol. 17, No. 1, pp. 105–110, 2002.

[7] H. Dommel, ElectroMagnetic Transients Program, BPA, Portland, Oregon, 1986.